EFFECTS OF LEO ENVIRONMENT ON MECHANICAL PROPERTIES OF POLYIMIDE FILMS UNDER TENSILE STRESS

Hiroyuki SHIMAMURA[1]

[1] *Institute of Aerospace Technology, Japan Aerospace Exploration Agency, Tsukuba, Ibaraki 305-8505, Japan*

Mechanical properties of polyimide films after exposure to a low earth orbit (LEO) environment were investigated using tensile tests. Polyimide films were placed in a tensile stress state during space exposure to evaluate the effects of tensile stress state on degradation of mechanical properties. Atomic oxygen (AO), ultraviolet (UV), and electron beam (EB) irradiation tests were also conducted for polyimide films to enable comparison to the degradation behavior of the flight samples. Results show that the tensile strength and elongation were decreased by space exposure. The reduction of the mechanical properties became marked as the exposure period increased. The AO irradiation was considered to be the main degrading factor; both UV and EB had only slight effects on the mechanical properties. The tensile strength and elongation of the AO irradiated samples decreased with increased AO fluence. Moreover, the surface roughness of the AO irradiated samples developed dependently on the increased AO fluence. Consequently, surface roughness is one of the leading causes of degradation of mechanical properties. Excessive stress might concentrate at a concave region on the rough surface, leading to formation of surface cracks and initiation points of destruction. No obvious difference attributable to the tensile stress state (below 7 MPa) was apparent in the degradation of mechanical properties.

Keywords: MPAC&SEED, Polyimide film, Mechanical property, Atomic oxygen, Surface roughness

1. Introduction

Space environmental factors such as orbital thermal cycling, high-energy ultraviolet (UV) and various types of radiation (protons, electrons, and X-rays) can strongly impact the performance of polymer materials used on spacecrafts. Thermal cycling accumulates heat strain in polymer materials, causing geometric variation, delamination, and cracks. Generally, a polymer material irradiated by UV or radiation changes its chemical construction with decompositions and cross-links of polymer bonds. The chemical construction change engenders brittleness and discoloration. In a low earth orbit (LEO), polymer materials exposed to a space environment are also degraded by atomic oxygen (AO). When a polymer material collides with AO at high velocity of about 8 km/s, its surface is deeply eroded by oxidative decomposition and a gasification reaction [1]. Then the polymer material thins and exhibits a rough texture, changing the optical reflectance of the material from specular to diffuse. The surface texture change increases the solar absorptance, which is an important parameter for a spacecraft's thermal control. Additionally, the surface texture can cause crack initiation and tearing of thin polymer films [2].

Among polymer materials, polyimide has considerable resistance to high temperatures and can function well in large operating temperature ranges; it also has a large tolerance against intense UV and radiation. For those reasons, polyimide has been applied predominantly to thermal control films such as the outermost layer film of multilayer insulation (MLI). The thermal control films are attached where they are exposed to a space environment. For thermal control applications, it is important to evaluate the degradation of thermo-optical properties by space exposure. Space exposure experiments and ground simulations for investigation of thermo-optical properties degradation have collected many data and have facilitated estimation of the degree of degradation in some orbits [3–5].

Polyimide has also been applied as a base film of deployable structures of spacecraft, such as large flexible solar arrays, large deployable antenna and solar sails, because of its high specific strength and rigidity, high dimensional accuracy, and low rate of thermal expansion [6–9]. Base films are used under tensile stress states to maintain their structural shapes at low gravity when deployable structures are fully expanded [10]. The initial tensile stress state is expected to be altered by orbital thermal cycling. For application as a structural material, it is indispensable to evaluate the space environmental effects on mechanical properties. The impacts of tensile stress states should also be understood if they hasten degradation of mechanical properties in a space environment.

Mechanical properties of polyimide films exposed to space environments have been studied in the Long Duration Exposure Facility (LDEF) experiment and the Materials International Space Station Experiment (MISSE) [11, 12]. Results of these experiments indicated that space exposure can degrade the mechanical properties of polyimide films. However, these experiments include large variations in their results. Another problem is that the sample number is insufficient to support statistical significance. Further study is needed to confirm which space environmental factors impart serious damage to mechanical properties, the extent to which degradation proceeds, and whether or not the tensile stress state affects the degradation.

In this study, polyimide films under a tensile stress state were exposed to a space environment with the Micro-Particles

Capturer and Space Environment Exposure Device on the International Space Station Russian Service Module (SM/MPAC&SEED); the polyimide films were included in the SM/SEED experiment samples. The overview of the experiment is described in [13]. Polyimide films were also irradiated by AO, UV, and electron beams (EB) in ground reference tests. After the space exposure and the ground reference tests, tensile tests of samples were conducted to evaluate changes of mechanical properties.

This paper reports the tensile test results of polyimide films after space exposure and each irradiation test. Then, the main space environmental factor affecting the mechanical properties of polyimide films are investigated through comparison of the sample's degradation behavior. Degradation mechanism of mechanical properties and effects of tensile stress state on the degradation are also discussed.

2. Experimental Procedures

2.1 Material

The tested polyimide films were 125-μm-thick UPILEX-S (UBE Industries Ltd.); UPILEX-S has been applied as a base film for the flexible solar array of the Space Flyer Unit (SFU) and the Advanced Earth Observing Satellite-I and II (ADEOS-I and II).

The sample dimensions are presented in Fig. 1. The sample has a dog-bone-shape which resembles the "Type IV" specimen of American Society for Testing and Materials (ASTM) Standard D-638-03 [14], punched out from a sheet using a die. For polymer sheet production, sheets are drawn to the rolling direction and polymer chains are aligned in the same direction. Then, tensile strength and elongation depend on the drawing direction. Therefore, the longitudinal direction of all samples was arranged to the drawing direction to prevent the influence of anisotropy.

As described above, a polymer material is eroded by AO attacks and thins with increased exposure. Before the beginning of the SM/SEED experiment, the sample erosion depth during the experimental duration of approximately 3 years was estimated at about 250 μm from the total AO fluence, which was calculated by the Space Environments and Effects System (SEES) simulation. For the 125-μm-thick polyimide film, a single layer is completely eroded away during the experiment. Additionally, the retrieval date can be delayed; then the samples are exposed to LEO environment much longer than the planned duration. Therefore, the flight samples consisted of four stacked layers to survive the SM/SEED experiment; total thickness of the stacked layers was 500 μm. The samples for ground reference tests have same configuration as the flight samples.

2.2 Tensile stress states

During the SM/SEED experiment and the ground reference tests, the samples were mounted on a tension-loading mechanism. Figures 2 and 3 show post-flight photographs of the tension-loading mechanism used in the SM/SEED experiment and a cross-sectional schematic view of the mechanism, respectively. The mechanism can apply unidirectional tensile stress to samples by pulling one end of the sample using a spring. The tensile stress applied to the samples was set to 0 MPa, 1.4 MPa, and 7.0 MPa by adjusting the spring elongation. The tensile stress level of 1.4 MPa was based on the nominal stress of the base films of the ADEOS-I solar paddles; 7.0 MPa was set five times as large as 1.4 MPa.

2.3 SM/SEED experiment

The SM/SEED experiment has three periods of exposure to a LEO environment: 315 days, 865 days, and 1403 days [13]. The first, second and third retrieval samples are designated as Flight #1, Flight #2, and Flight #3 in this paper, respectively.

The polyimide films mounted on a tension-loading mechanism were set in the RAM side of the SM/MPAC&SEED unit, as presented in Fig. 4. The number of the flight samples was two for each tensile stress state.

The estimated environmental conditions for the flight samples on the RAM side are shown in Table 1. The AO and UV fluence and the total ionizing dose for the flight samples resulted from the evaluations of monitoring samples, which were mounted on the SM/SEED experiment, and SEES simulations [15].

Table 1 Environmental conditions for the flight samples [15]

		Flight #1	Flight #2	Flight #3
Exposure duration, days		315	865	1403
AO fluence, atoms/cm^2	Vespel	2.04×10^{20}	2.57×10^{20}	2.70×10^{20}
	SEES	2.85×10^{21}	5.70×10^{21}	8.41×10^{21}
UV fluence, ESD*	Polyurethane	18.1	15.8	13.4
	SEES	73.8	167	271
Total ionizing dose**, Gy	Alanine dosimeter	1.95	15.3	32.0
	SEES	67.6	181	234
Maximum temperature***, °C		60	90	90

* Equivalent Solar Day, 1 ESD = 1.02×10^7 J/m^2

** Shield thickness; 0.04 g/cm^2

*** Temperature at approximately 1 mm depth

2.4 Ground reference irradiation tests

In ground reference tests, the samples were irradiated by AO, UV, and EB. Respective irradiation test conditions are presented in Tables 2, 3, and 4.

The AO irradiation testing was performed using the "Combined Space Effects Test Facility" of JAXA Tsukuba Space Center [16]. This facility has a laser detonation AO beam source. The AO velocity was controlled to approximately 8 km/s to simulate the LEO environment; the translational energy was 5 eV at the velocity. Kapton H (DuPont) films were adopted as AO monitoring sample with a well-known erosion yield of 3.0×10^{-24} cm^3/atom [17]. The AO fluence was estimated from the mass loss of Kapton H after AO irradiation tests using the following equation.

$$F = \frac{\Delta m_K}{A_K \rho_K E_K} \quad (1)$$

where

F = total AO fluence
Δm_K = mass loss of Kapton H
A_K = exposure area of Kapton H
ρ_K =density of Kapton H
E_K = erosion yield of Kapton H, 3.0×10^{-24} cm^3/atom [17]

A high-vacuum chamber equipped with a Xe lamp was used for UV irradiation tests. The UV flux and fluence levels at a wavelength of 200–400 nm were measured using a multispectral radiometer. The Xe lamp light includes an infrared wavelength region. Then samples are expected to be heated during UV irradiation. Therefore, the backsides of the samples were cooled by water flow to prevent sample heating. The temperature of the sample surfaces was monitored using thermocouples.

The Combined Space Effects Test Facility was also used for EB irradiation tests. The accelerating voltage and the electron current for the irradiation tests were set at 200 kV and 2.0 mA, respectively. The total doses for samples were monitored by cellulose triacetate (CTA) films mounted with irradiated samples.

Table 2 AO irradiation test conditions

AO flux, atoms/cm^2·s	1.0–5.0 × 10^{15}
AO fluence, atoms/cm^2	0.3 × 10^{21} 1.3 × 10^{21} 4.1 × 10^{21}
AO velocity, km/s	8.0
Vacuum, Pa	10^{-2}–10^{-3}

Table 3 UV irradiation test conditions

UV flux, ESD*/day	10
UV fluence, ESD*	20 35 69
Sample surface temperature, °C	10–30
Vacuum, Pa	10^{-4}–10^{-5}

* Equivalent Solar Day, 1 ESD = 1.02 × 10^7 J/m^2

Table 4 EB irradiation test conditions

EB dose, kGy (Irradiation time, s)	1.6 (26) 3.3 (53)
Vacuum, Pa	10^{-4}–10^{-5}

2.5 Calculation of thickness change

Thickness changes of each sample were calculated using the following equation from the mass loss after space exposure or ground reference tests:

$$\Delta t_S = \frac{\Delta m_S}{A_S \rho_S}, \qquad (2)$$

where

Δt_S = thickness loss of samples
Δm_S = mass loss of samples
A_S = exposure area of samples
ρ_S =density of samples
(UPILEX-S: 1.47 g/cm^3 [18])

2.6 Tensile tests

Mechanical properties of samples were evaluated by tensile testing using Autograph AG-5kNI (Shimadzu Corp.) and Instron 5565 (Instron Corp.). Four-layer stacked samples were used for tensile tests. Grip sections of the samples were mutually bonded using an adhesive to prevent interlayer slippage during tensile tests. Before testing, tensile tests results for stacked samples were compared to that for one-layer samples in order to confirm that tensile tests using stacked samples can properly evaluate tensile characteristics of samples. In consequence, no difference was apparent between stress-strain curves of four-layer stacked samples and those of one-layer samples.

Tensile tests were conducted according to ASTM D-638-03 [14], at room temperature and 50±5% relative humidity under a constant strain rate of 50 mm/min. The strain was obtained based on the crosshead travel distance. The tensile strength and elongation were determined as the maximum stress and the strain at the first failure of four-layer stacked films, respectively. For the calculation of tensile strength, the thickness loss defined by Eq. (2) was considered.

3. Results and Discussion

The thickness loss of flight samples is expected to become larger with increased exposure duration. There is, however, no remarkable difference of the thickness loss among flight samples, as presented in Fig. 5. In addition, the thickness loss of Flight #3 was about 8 μm, a much lower than expected value, which is approximately 250 μm for three years of space exposure. In ground reference tests, only AO irradiation decreased the sample thickness; there was almost no variation in the mass of UV and EB irradiated samples. The thickness loss of AO irradiated samples increased in direct relation to AO fluence in Fig. 6. No considerable change attributable to tensile stress state was found in either the flight or AO-irradiated samples.

Tensile strength and elongation changes of the flight samples for exposure duration are portrayed in Fig. 7. The tensile strength of the flight samples had decreased slightly from the value of control samples. A major reduction in elongation was detected, showing 70% loss compared to the control samples at a maximum. Samples of Flights #2 and #3 showed more serious degradation than Flight #1 in both tensile strength and elongation.

The AO irradiated samples deteriorated considerably with increasing AO fluence, as portrayed in Fig. 8. The samples at AO fluence of 4.1 × 10^{21} atoms/cm^2 showed a large reduction of 40% in tensile strength and a reduction of 80% in elongation compared to the control samples, which indicated considerable degradation as a polymer material. Both tensile strength and elongation at AO fluence of 0.3 × 10^{21} atoms/cm^2 are within the deviation of control samples. According to this result, AO irradiation cannot affect mechanical properties of polyimide films at low fluence.

As shown in Fig. 9, minor changes of tensile strength and elongation occurred in UV irradiated samples. Because polyimides have a high absorption in the UV region, UV irradiation causes extensive surface degradation, leaving the inside intact [19]. Therefore, it is conceivable that UV irradiation imparted no considerable deleterious effect on mechanical properties of polyimide films.

In addition, EB irradiation little affected tensile strength and elongation of polyimide films, as shown in Fig. 10. Generally, polyimide has a high concentration of imide rings in the main chain, rendering it resistant to EB irradiation because of pi-electron conjugation. The EB dose level, by which the elongation of UPILEX-S declines to 50% of its initial value, is approximately 30 MGy [20]. The dose levels in present EB irradiation tests, 1.6 kGy and 3.3 kGy, are extremely small compared to 30 MGy. Therefore, noticeable degradation of mechanical properties by EB irradiation was not detected at these EB dose levels.

For the flight and ground reference samples, there was no marked difference depending on the tensile stress state in tensile strength and elongation. This result means that a tensile stress state of less than 7.0 MPa has no impact on polyimide films' degradation of mechanical properties. The tensile stress of 7.0 MPa is only a few percent of the yield stress of control samples. It is conceivable that the tensile stress states used for this study are too weak to degrade samples. Further experiments using higher stress are needed to clarify the effects of tensile stress state on the degradation of mechanical properties of polyimide films. This result, however, demonstrated that the practical tensile stress states for spacecrafts contribute no degradation of the mechanical properties.

Ground reference tests showed considerable degradation of mechanical properties of polyimide films only in AO-irradiated samples. Consequently, AO irradiation is considered to be the main degrading factor for mechanical properties. In addition, according to the fact that the degradation became noteworthy only with the AO fluence increase, as presented in Fig. 8, it can be argued that mechanical properties of polyimide films degrade with increased space exposure duration, but that the tensile strength and elongation of Flight #3 are nearly equal to those of Flight #2, as shown in Fig. 7.

The degradation behavior of flight samples for AO fluence is compared to that of the AO irradiated samples in Fig. 11, which shows the tensile strength and elongation for the samples under a no-tensile-stress state. Flight samples were plotted for two kinds of AO fluence: one is determined by the analysis of the AO monitoring sample on the SM/SEED experiment; the other is estimated by the simulation using SEES [15]. An enormous discrepancy pertains between these two kinds of AO fluence. The tensile strength and elongation of flight samples were decreased as the AO fluence increases, denoting the same tendency of the AO irradiated samples. However, it is difficult to interpret the consistency of the degree of degradation between the flight samples and the AO irradiated samples because of the large discrepancy of the flight samples' AO fluence.

The flight sample surfaces that had been exposed to the space environment were observed using SEM, as presented in Fig. 12. The samples were tilted 45 degrees to facilitate viewing of the surface topography. All flight sample surfaces showed a rough texture, which is typical for an AO-irradiated polyimide [1]. No obvious differences between Flight #1, #2, and #3 were detected in surface texture, even though these flight samples had different exposure durations. Some contamination was visible on all flight samples' surfaces.

The other samples on SM/SEED were also contaminated by outgassing from organic materials used in the ISS; the main components of contamination were found to be SiO_x [21, 22]. The SiO_x contamination layer on the flight sample surface can serve as the anti-AO coating; the flight samples were prevented from AO erosion because of the contamination layer. As described above, the thickness losses of each flight sample were far below the expected value. Moreover, thickness loss and surface texture of flight samples were approximately equivalent, irrespective of the space exposure duration. These phenomena stem from the SiO_x contamination layer.

The contamination thickness for Flight #3 was estimated as about 120 nm [21], which is quite small compared to the amount of thickness loss for the flight samples. Consequently, the mass increase by contamination attachment is sufficiently smaller than the mass loss by AO erosion. Therefore, the influence of contamination attachment is negligible in the thickness loss calculation using Eq. (2).

The surface topography of AO irradiated samples was also evaluated with SEM observation at a 45-degree tilt, as presented in Fig. 13. The sample surfaces were deeply eroded by AO irradiation, exhibiting a rough texture. The surface roughness of the AO irradiated sample, 1.3×10^{21} atoms/cm^2, was remarkable compared to that of the AO irradiated sample, 0.3×10^{21} atoms/cm^2. This result indicates that surface roughness develops as AO fluence increases. The relation between the roughness of the AO irradiated surface and AO fluence has been investigated through surface observations using SEM or AFM, or Monte Carlo computational modeling [23–25]. Our current results are consistent with past investigation results.

Results of SEM observation revealed that the amount of surface roughness increases concomitant with the AO fluence. In addition, the degradation of tensile strength and elongation of samples was enhanced by increasing AO fluence, as presented in Fig. 8. From these results, surface topography transformation to greater roughness might correlate with the degradation of tensile strength and elongation. It is generally assumed that excessive stress concentrates at a concave region on the rough surface during deformation; then the concave region can develop into surface cracks and become the initiation point of the polymer film's destruction. The increased surface roughness facilitates crack formation and hastens destruction.

Flight #3 showed a significant decrease that was greater than that of the AO irradiated sample of 1.3×10^{21} atoms/cm^2, as presented in Fig. 11. Nevertheless, a broad distinction of surface topography was made between Flight #3 and the AO irradiated sample of 1.3×10^{21} atoms/cm^2, as revealed by surface observations using SEM; the surface roughness of Flight #3 was a much lower than that of the AO irradiated sample of 1.3×10^{21} atoms/cm^2. Then, cross-section observation was conducted to identify the surface topography for Flight #3. The samples for cross-section observation were embedded in epoxy and then cut with a microtome.

The three cross-sections for Flight #3 under no tensile stress during space exposure are presented in Fig. 14. The boundary between the sample and the embedding agent is traced in Fig. 14 to clarify the surface texture. Numerous blunt and short cones are formed on the Flight #3 surface. The average surface roughness, R_z, was approximately 1 μm. It should be noted that the Flight #3 surface exhibits some extremely deep concavities compared to its surroundings, as indicated by the white arrow in Fig. 14. Stress can readily concentrate at the deep concavities compared with surroundings; these deep concavities can exert a large reduction in mechanical properties of Flight #3.

4. Conclusions

Degradation of mechanical properties for polyimide films exposed to a LEO environment was investigated using tensile tests. Some polyimide films were under a tensile stress state during space exposure to evaluate the effects of the tensile stress state on degradation.

The tensile strength and elongation of polyimide films decreased during space exposure. The reduction of the mechanical properties became marked as the exposure period increased. Ground reference tests demonstrated that the AO irradiated samples underwent considerable degradation of tensile strength and elongation; the samples exhibited no marked degradation of mechanical properties by either UV or EB. This result clearly suggests that AO attack is the main cause of decreased tensile strength and elongation in a LEO environment. A tensile stress state of less than 7.0 MPa, which was applied to the samples during space exposure and irradiation tests, had little effect on the degradation of the mechanical properties of any sample.

The tensile strength and elongation were decreased with increased AO fluence. In addition, the surface roughness developed dependently on the increased AO fluence. Consequently, the rough surface was regarded as a cause of degradation of mechanical properties. It is generally assumed that excessive stress concentrates at a concave region on the rough surface during deformation, leading to formation of surface cracks and initiation points of destruction.

The flight samples' surfaces showed a rough texture by AO erosion. Additionally, some extremely deep concavities compared to surroundings were found on the surface. These deep concavities have the potential to reduce mechanical properties considerably.

Acknowledgments

The author gratefully acknowledges the experimental support of the Advanced Engineering Services staff, and greatly appreciates the work of all people involved in the development and operation of the SM/MPAC&SEED project.

References

[1] R. C. Tennyson, "Atomic Oxygen and Its Effects of Materials," *The Behavior of Systems in the Space Environment*, edited by R. N. DeWitt, Kluwer Academic, Amsterdam, 1993, pp. 233–357.

[2] Bruce A. Banks, Aaron Snyder, and Sharon K. Miller, "Issues and Consequences of Atomic Oxygen Undercutting of Protected Polymers in Low Earth Orbit," NASA TM-211577, 2002.

[3] Joseph Marco and Stephanie Remaury, "Evaluation of Thermal Control Coatings Degradation in Simulated Geo-Space Environment," *High Performance Polymers*, Vol. 16, 2004, pp. 177–196.

[4] Youichi Nakayama, Kichiro Imagawa, Minoru Tagashira, Muneaki Nakai, Hisaaki Kudoh, Masaki Sugimoto, Noboru Kasai, and Tadao Seguchi, "Evaluation and Analysis of Thermal Control Materials under Ground Simulation Test for Space Environment Effects," *High Performance Polymers*, Vol. 13, 2001, pp. S433–S451.

[5] Edward M. Silverman, "Space Environment Effects on Spacecraft: LEO Materials Selection Guide," NASA Contractor Report4661 Part 1 & 2, 1995.

[6] Mark J. Forkapa, Curtis R. Stidham, Bruce A. Banks, Sharon K. Rutledge, David H. Ma, and Edward A. Sechkar, "Atomic Oxygen Durability Testing of an International Space Station Solar Array Validation Coupon," NASA TM-107212, 2001.

[7] Y. Shibayama, H. Arai, K. Matsui, K. Hama, A. Ushirokawa, M. Natori, K. Takahashi, N. Wakasugi, and T. Anzai, ""SFU" Solar Array," *Proceedings of European Space Power Conference*, Madrid, Oct, 1989.

[8] http://www.jaxa.jp/press/2004/05/20040521_midori2-03_j.pdf (in Japanese)

[9] Yuichi Tsuda, Osamu Mori, Shinsuke Takeuchi, and Junichiro Kawaguchi, "Flight Result and Analysis of Solar Sail Deployment Experiment Using S-310 Sounding Rocket," *Proceedings of 56th International Astronautical Congress* [CD-ROM], Fukuoka, Japan, 17–21 Oct., 2005.

[10] David L. Edwards, William A. Hollerman, Whitney S. Hubbs, Perry A. Gray, George E. Wertz, David T. Hoppe, Mary K. Nehls, and Charles L. Semmel, "Electron Radiation Effects on Candidate Solar Sail Materl," *High Performance Polymers*, Vol. 16, No. 2, 2004, pp. 277–288.

[11] J. B. Whiteside, D. Giangano, R. L. Heuer, E. Kamykowski, M. Kesselman, W. D. Rooney, R. Schulte, and M. Stauber, "Effects of the Space Environment on Space-Based Radar Phsed-Array Antenna; Status and Preliminaly Observations (LEDF Experiment A0133)," *Proceedings of LDEF-69 Months in Space First Post-Retrieval Symposium*, Kissimmee, Florida, 2–8 June, 1991.

[12] Joyce A. Dever, Sharon K. Miller, and Edward A. Sechlar, "Effects of the Space Environment on Polymer Film Materials Exposed on the Materials International Space Station Experiment (MISSE 1 and MISSE 2)," *Proceedings of the 10th International Symposium on "Materials in a Space Environment" & the 8th International Conference on "Protection of Materials and Structures in a Space Environment"* [CD-ROM], Collioure, France, 19–23 June, 2006.

[13] Yugo Kimoto, Junichiro Ishizawa, Eiji Miyazaki, and Mineo Suzuki, "SM/MPAC&SEED Experiment Overview," *Proceedings of International Symposium on "SM/MPAC&SEED Experiment,"* Tsukuba, Japan, 10–11 March, 2008.

[14] American Society for Testing and Materials (ASTM) Standard D-638-03, "Standard Test Method for Tensile Properties of Plastics," 2003.

[15] Yugo Kimoto, Keiichiro Yano, Junichiro Ishizawa, and Eiji Miyazaki, "Post Retrieval Analyses of Space Environment Monitoring Samples: Radiation Effects, UV, and Atomic Oxygen Fluence," *Proceedings of International Symposium on "SM/MPAC&SEED Experiment,"* Tsukuba, Japan, 10–11 March, 2008.

[16] Yasuo Tanaka, Masanori Iwaki, Singo Obara and Hiroyuki Nagata, "New High Vacuum Test Facilities for Mechanical Components (part 1) -UHV Surface Properties Test Facility and Combined Space Effects Test Facility," *Proceedings of 21st International Symposium on Space Technology and Science*, 1998.

[17] American Society for Testing and Materials (ASTM) Standard E-2089-00, "Standard Practices for Ground Laboratory Atomic Oxygen Interaction Evaluation of Materials for Space Application," 2000.

[18] UBE Industries, ltd., UPILEX-S Catalog.

[19] David J. T. Hill, Firas A. Rasoul, John S. Forsythe, James H. O'Donnell, Peter J. Pomery, Graeme A. George, Philip R. Young, and John W. Connell, "Effect of Simulated Low Earth Orbit Radiation on Polyimides (UV Degradation Study)," *Journal of Applied Polymer Science*, Vol. 58, 1995, pp. 1847–1856.

[20] Tsuneo Sasuga, Naohiro Hayakawa, Kenzo Yoshida, and Miyuki Hagiwara, "Degradation in Tensile Properties of Aromatic Polymers by Electron Beam Irradiation," *Polymer*, Vol. 26, 1985, pp. 1039–1045.

[21] Eiji Miyazaki, Junichiro Ishizawa and Hiroyuki Shimamura, "Evaluation of F-OSR Exposed to Space on SM/SEED Experiment," *Proceedings of International Symposium on "SM/MPAC&SEED Experiment,"* Tsukuba, Japan, 10–11 March, 2008.

[22] Naoko Baba, and Yugo Kimoto, "Contamination Effect on SM/MPAC&SEED Experiment," *Proceedings of International Symposium on "SM/MPAC&SEED Experiment,"* Tsukuba, Japan, 10–11 March, 2008.

[23] Deborah L. Waters, Bruce A. Banks, Stephen D. Thorson, Kim K. de Groh and Sharon K. R. Miller, "Comparison of the Atomic Oxygen Erosion Depth and Cone Height of Various Materials at Hyperthermal Energy," *Proceedings of the 10th International Symposium on "Materials in a Space Environment" & the 8th International Conference on "Protection of Materials and Structures in a Space Environment"* [CD-ROM], Collioure, France, 19–23 June, 2006.

[24] R. Vered, G. D. Lempert, E. Grossman, Y. Haruvy, G. Marom, L. Singer, and Y. Lifshitz, "Atomic Oxygen Erosion of Teflon FEP and Kapton by Oxygen from Different sources: Atomic Force Microscopy and Complementary Studies," *Proceedings of the 6th International Symposium on "Materials in a Space Environment,"* Noordwijk, The Netherlands, 19–23 September, 1994.

[25] Bruce A. Banks, Thomas J. Stueber, Scott A. Snyder, Sharon K. Rutledge, and Mary J. Norris, "Atomic Oxygen Erosion Phenomena," AIAA-1997-3903, 1997.

Publication list related SM/MPAC&SEED

1. Hiroyuki Shimamura, and Ichiro Yamagata, "Degradation of Tension-Loaded Polyimide Films in a Space Environment: Results of the SM/MPAC&SEED Mission," *Proceedings of the 10th International Symposium on "Materials in a Space Environment" & the 8th International Conference on "Protection of Materials and Structures in a Space Environment"* [CD-ROM], Collioure, France, 19–23 June, 2006.
2. Hiroyuki Shimamura and Takashi Nakamura, "Evaluation of Tension-Applied Polyimide Films Exposed to Space Environment on ISS Russian Service Module/Space Environment Exposure Device," *Proceedings of 51st Space Sciences and Technology Conference*, Sapporo, Japan, 29–31 October, 2007. (in Japanese)

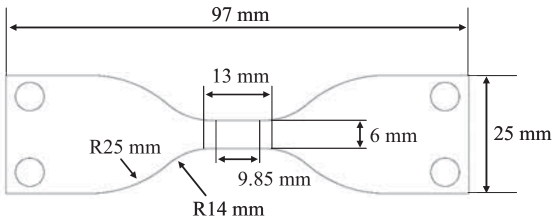

Fig. 1 Schematic view of the sample.

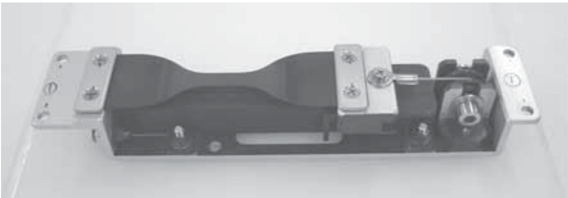

Fig. 2 Post-flight photograph of the tension-loading mechanism with a sample.

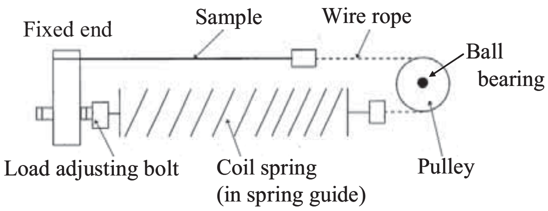

Fig. 3 Cross-sectional view of the tension-loading mechanism.

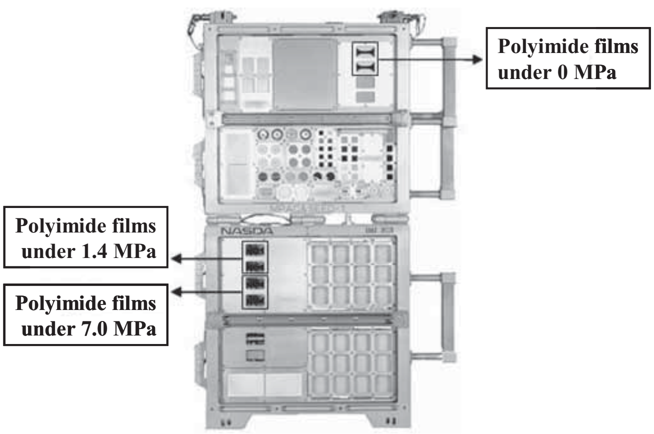

Fig. 4 Mounting location of polyimide films in the RAM side of the SM/MPAC&SEED unit.

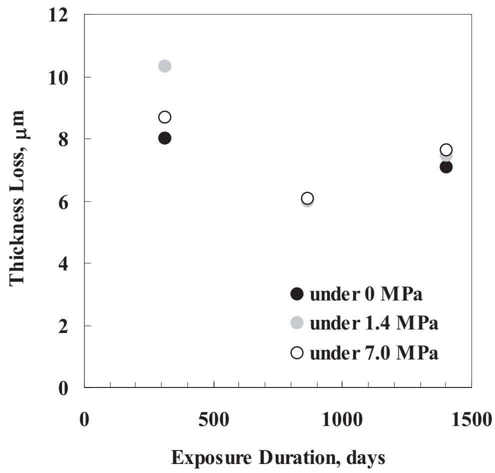

Fig. 5 Thickness loss of the flight samples.

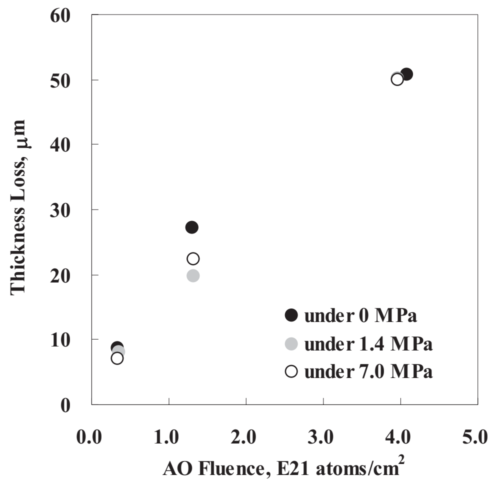

Fig. 6 Thickness loss of the AO irradiated samples.

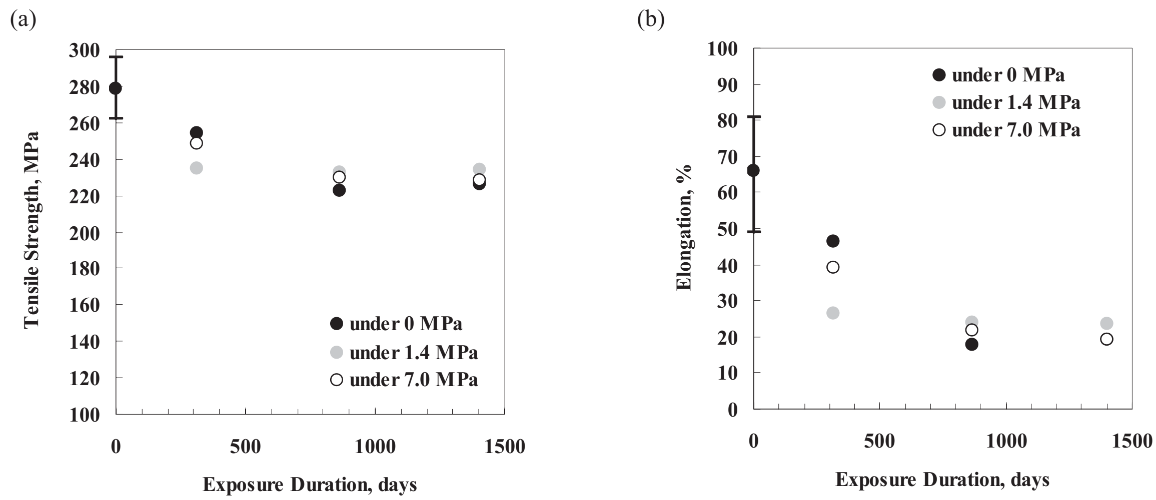

Fig. 7(a) Tensile strength and (b) elongation of the flight samples.

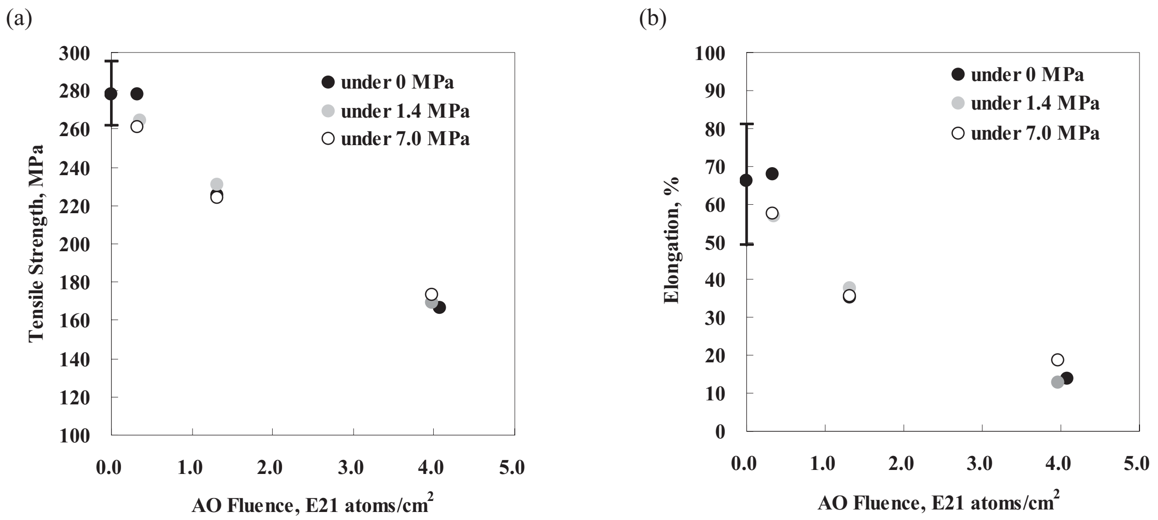

Fig. 8(a) Tensile strength and (b) elongation of the AO irradiated samples.

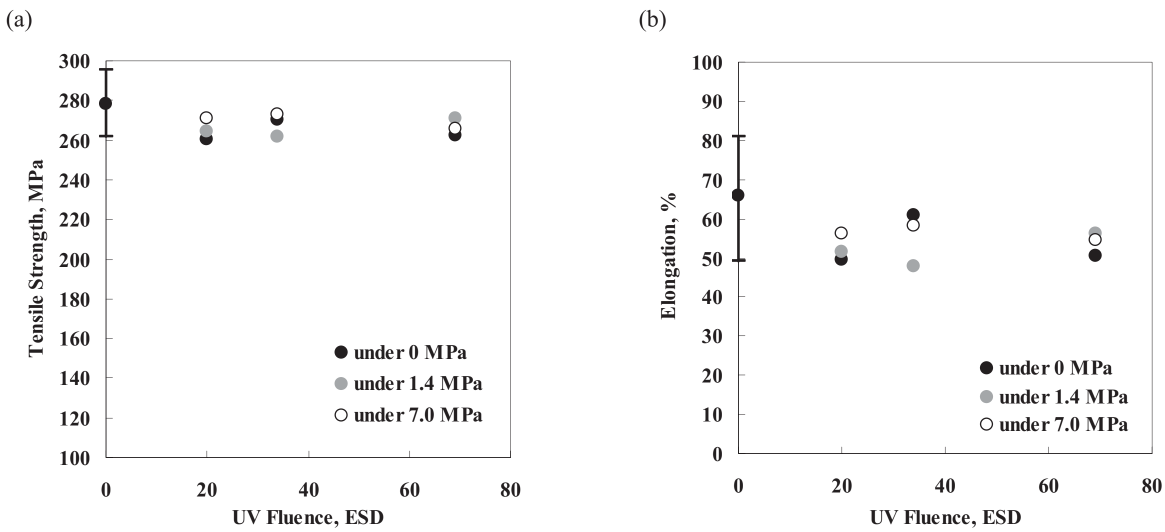

Fig. 9(a) Tensile strength and (b) elongation of the UV irradiated samples.

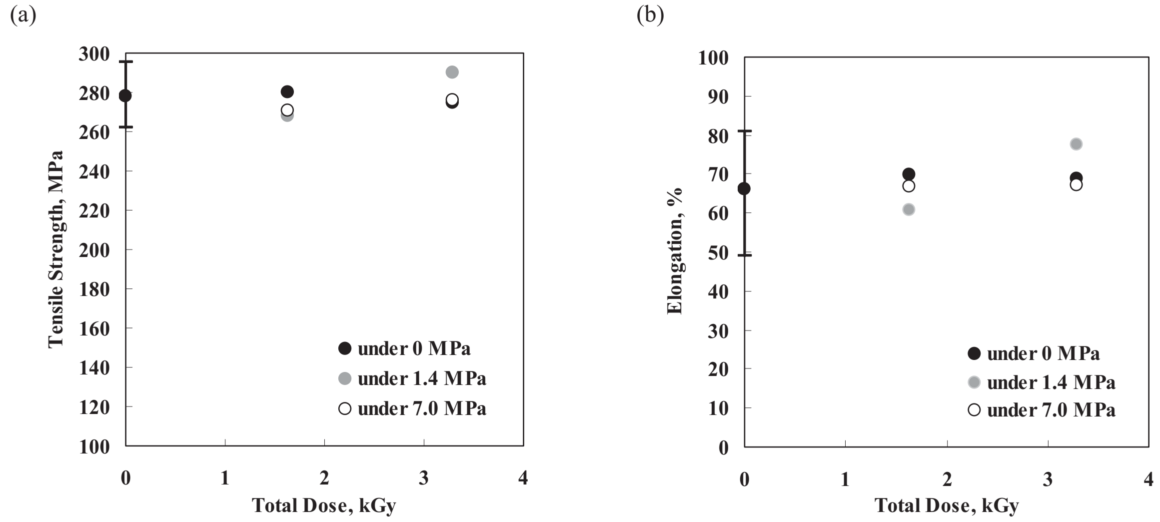

Fig. 10(a) Tensile strength and (b) elongation of the EB irradiated samples.

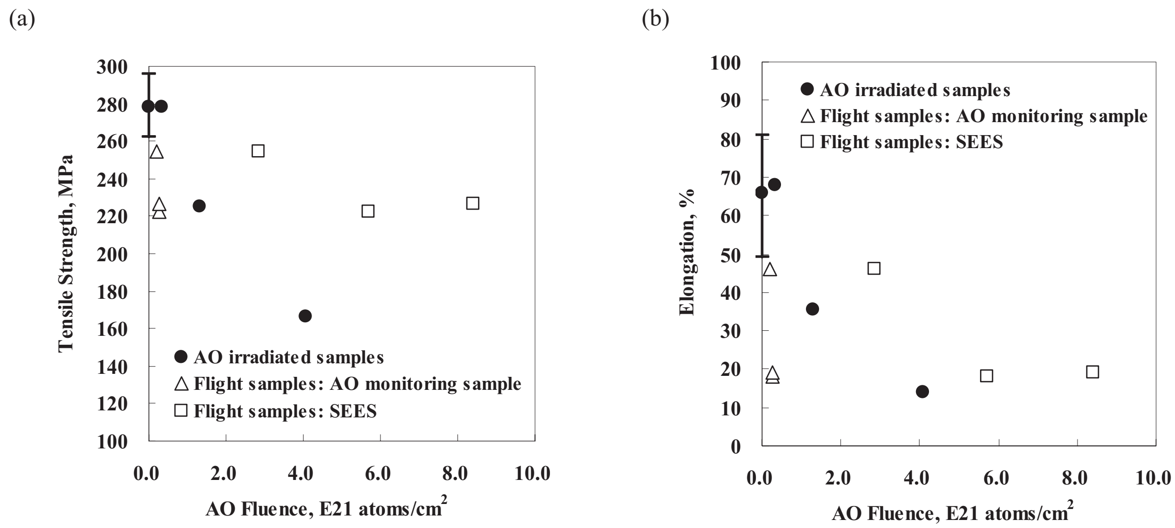

Fig. 11 (a) Tensile strength and (b) elongation of flight samples and AO irradiated samples for AO fluence. These figures show data for the samples under no tensile stress. Flight samples were plotted for two kinds of AO fluence: one is determined by the analysis of the AO monitoring sample on the SM/SEED experiment; the other is estimated by the simulation using SEES [15]

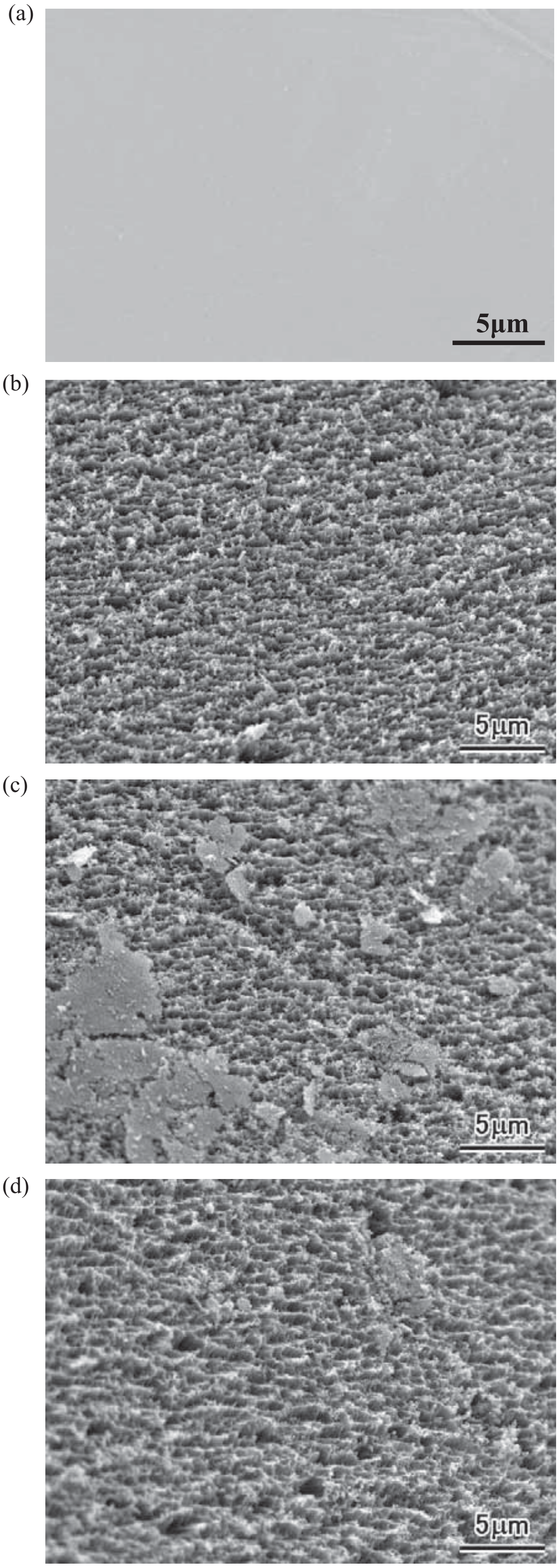

Fig. 12 SEM images of (a) the control sample, (b) Flight #1 and (c) Flight #2, and (d) Flight #3. The flight samples were under no tensile stress state during space exposure.

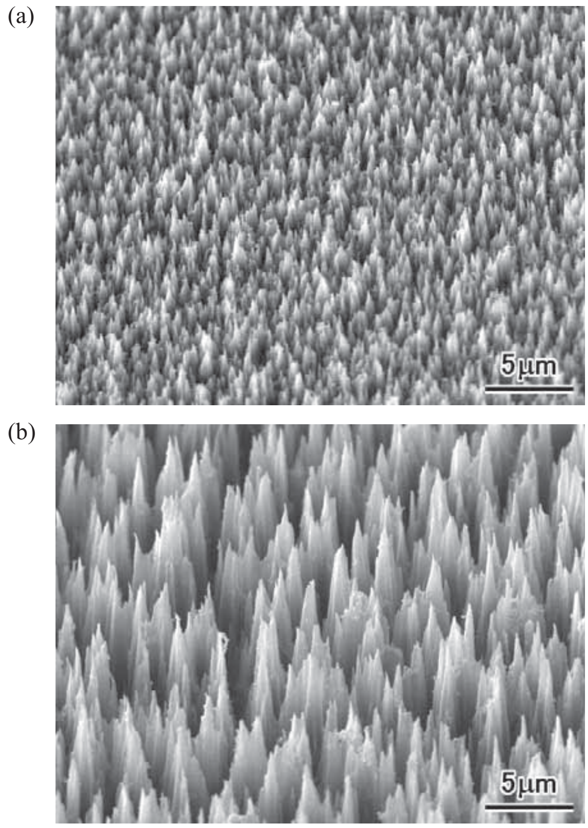

Fig. 13 SEM images of (a) the AO irradiated sample at 0.3 × 10^{21} atoms/cm^2 and (b) the AO irradiated sample at 1.3 × 10^{21} atoms/cm^2. These samples were under no tensile stress during AO irradiation tests.

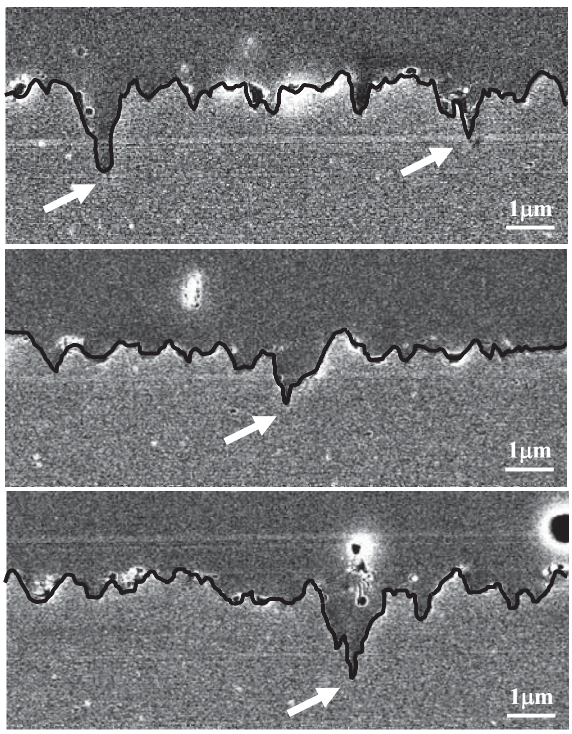

Fig. 14 Cross-sections of Flight #3 under no tensile stress during space exposure. The boundary between the sample and the embedding agent was traced to clarify the surface aspect.